Microscopic origin of light-induced ESR centers in undoped hydrogenated amorphous silicon

Takahide Umeda[1,2,*] Satoshi Yamasaki,[1] Junichi Isoya,[1,3] and Kazunobu Tanaka[1,2]

[1]*Joint Research Center for Atom Technology (JRCAT)–National Institute for Advanced Interdisciplinary Research (NAIR),*
Tsukuba,305-8562, Japan
[2]*Institute of Materials Science, University of Tsukuba, Tsukuba, 305-0006, Japan*
[3]*University of Library and Information Science, Tsukuba, 305-0821, Japan*
(Received 12 March 1999; revised manuscript received 2 May 2000)

^{29}Si hyperfine (hf) structures of light-induced electron-spin-resonance (LESR) centers of $g = 2.004$ and 2.01 have been investigated in undoped hydrogenated amorphous silicon (a-Si:H) with different ^{29}Si content (1.6, 4.7,9.1 at. %) by means of pulsed and multifrequency (3,11,34 GHz) ESR techniques. We have experimentally deconvoluted overlapping LESR signals using the difference in the spin-lattice relaxation time between the two signals. The deconvoluted ^{29}Si hf structure of $g = 2.004$ indicates that the wave function of the $g = 2.004$ center spreads mainly over two Si atoms. Accordingly, we propose that the origin of $g = 2.004$ is electrons trapped in antibonding states of weak Si-Si bonds rather than those trapped at positively charged dangling bonds. The isotropic hf splittings were estimated to be around 7 mT for $g = 2.004$ and below 3 mT for $g = 2.01$, which are in good agreement with characteristics of the antibonding and bonding states of the weak Si-Si bond. We suggest, from our ^{29}Si hf data and other experimental findings, that the $g = 2.004$ center is localized spatially more than conduction-band-tail electrons detected by photoluminescence.

I. INTRODUCTION

In amorphous semiconductors, there exist band-tail states in the gap both just below the conduction band and above the valence band, which have been evidenced by the optical absorption spectrum,[1] photoemission spectra,[2] drift mobility–multiple trapping,[3] and modulated photocurrent spectroscopy.[4] The band-tail states are characterized as localized states and play an important role in transport and optical properties. It is widely accepted that those localized states originate from potential fluctuations due to variation in bond lengths, bond angles, and other topological parameters. However, there has been no experimental information available on the microscopic structure of the potential fluctuation.

In undoped a-Si:H, two light-induced electron-spin-resonance (LESR) signals of $g = 2.004$ and 2.01 have been detected at low temperatures.[5] Doped a-Si:H, e.g., phosphorus- and boron-doped a-Si:H, also shows $g = 2.004$ and 2.01 signals in the dark at low temperatures. In these samples the Fermi level shifts up to the conduction- and down to the valence-band tail in thermal equilibrium.[6–8] On the basis of doping, photoluminescence, and photoconductivity experiments, Street, Biegelsen, and Wiesfield concluded that the origins of those signals should be ascribed to conduction-band-tail electrons ($g = 2.004$) and valence-band-tail holes ($g = 2.01$).[7] Thus, the microscopic origins of these ESR centers are directly connected to microscopic information about the potential fluctuation of the band-tail states.

The microscopic origin of the LESR centers is also important to another unresolved issue: whether undoped a-Si:H films include a large number of charged dangling bonds (DB's) or not at thermal equilibrium. For example, chalcogenide glasses also show LESR signals at low temperatures, but almost no ESR signals are detected in the dark.[9] This has been interpreted in terms of negative effective correlation energy (U) for DB's, that is all DB's are considered to form pairs of positively and negatively charged DB's in thermal equilibrium.[9–11] In this model, naturally, the origins of the LESR signals are photoexcited electrons and holes trapped at the charged DB's.[9] In contrast, a-Si:H shows a pronounced dark ESR signal of $g = 2.0055$ that has been generally identified as a neutral DB signal.[12–14] It is therefore believed that a-Si:H is a positive-U material.[15] Further, this assignment is consistent with the sensitivity of the Fermi level to doping in a-Si:H.[8,16] However, several papers have argued the existence of a large number of charged DB's in thermal equilibrium, which is associated with the coexistence of negative and positive U.[17–20] In those papers, a carrier-trapped negative-U DB is one of the candidates for the origin of the LESR centers and possibly for the precursor of photocreated neutral DB's in the Staebler-Wronski effect.[17–20] Thus the LESR centers are related to a major unresolved problem in a-Si:H.

The microscopic origins of the 2.004 and 2.01 centers are expected to be revealed by detailed analyses of hyperfine (hf) structures of ^{29}Si (nuclear spin of $I = \frac{1}{2}$, natural abundance of 4.7 at. %) in the ESR spectrum. Yamasaki et $al.$ detected such ^{29}Si hf structures in the LESR spectrum of undoped a-Si:H using a pulsed ESR technique.[19] However, it was difficult to experimentally deconvolute the two overlapping LESR signals, which is necessary for extracting conclusive information about the ^{29}Si hf interactions. On the other hand, no discernible ^{29}Si hf structure has been found in doped a-Si:H owing to the interference with hf structures of the dopant atoms.[11,21]

Therefore, we directed our attention to the experimental deconvolution of ^{29}Si hf structures of LESR spectra in undoped a-Si:H. We found a difference in the spin-lattice relaxation time (T_1) between two LESR signals, which enables us to deconvolute the LESR signals experimentally. For the purpose of precise analysis of ^{29}Si hf interactions,

TABLE I. List of samples and their properties. Total and distant hydrogen content was determined by ^{1}H NMR measurements. The distant hydrogen was revealed by a narrow, Lorentzian component (full width at half maximum 10 kHz) in the ^{1}H NMR spectrum. Activation energy of the dark conductivity of the B-doped sample (E_a) was deduced from our previous data. (Ref. 23)

	Undoped		
$[^{29}\text{Si}]$ (at.%)	Total $[^1\text{H}]$ (at. %)	Distant $[^1\text{H}]$ (at. %)	N_{dark} (cm^{-3})
1.6	8.9	2.2	6×10^{15}
4.7	6.8	1.1	1×10^{15}
9.1	10.7	3.3	4×10^{15}
	B doped		
$[\text{B}_2\text{H}_6]/[\text{SiH}_4] = 0.89\%$		$E_a = 0.25 - 0.3$ eV	

undoped samples with different amounts of the ^{29}Si isotope (9.1,4.7,1.6 at. %) were prepared and subjected to pulsed ESR measurements. Prior to this paper, we published a brief report of our work.[22] This paper presents more detailed data and complete descriptions of the experiments and discussion. After the detailed description of experimental conditions (Sec. II), the spin-lattice relaxation of the LESR centers is elucidated by time-domain measurements of pulsed ESR (Sec. III A). Then, taking advantage of the difference in T_1, experimentally deconvoluted spectra of $g = 2.004$ and 2.01 are presented (Sec. III B). From ^{29}Si hf structures of the deconvoluted 2.004 and 2.01 spectra, detailed information about the electronic structures of the LESR centers is obtained (Sec. III C). Finally, we propose a weak Si-Si bond model to account for the origin of the LESR centers (Sec. IV A), and discuss this model in comparison with previous photoluminescence data (Sec. IV B).

II. EXPERIMENTAL DETAILS

Undoped a-Si:H samples were deposited by the conventional rf glow-discharge technique on aluminum foil at 250 °C. The ratio of ^{29}Si atoms to total Si atoms, p, was varied from 1.6 to 4.7 to 9.1 at. % for our samples. Flaked samples (1 to 2 μm in thickness, around 30 mg) were collected in a high-purity vitreous-silica tube (2.5 mm in inner diameter) for ESR measurements. We also prepared a boron-doped a-Si:H sample from a mixture of SiH$_4$ and B$_2$H$_6$ with $[\text{B}_2\text{H}_6]/[\text{SiH}_4] = 0.89\%$ at the deposition temperature of 250 °C. Dark spin densities (N_{dark}) and hydrogen contents of our samples are listed in Table I.

ESR spectra were measured by the echo-detected ESR technique of pulsed ESR to perform a variety of deconvolution procedures and to obtain wide-dynamic-range spectra. In the standard technique of echo-detected ESR, the spectrum is obtained by recording amplitudes of the two-pulse Hahn spin echo (90° pulse$-\tau-$180° pulse$-\tau-$echo, $\tau = 240$ nsec) as a function of magnetic-field strength.[19] At each magnetic field, a pulse sequence was repeated 1000 to 4000 times with an interval of RT (repetition time) which is generally set to be much longer than T_1. The T_1 value represents a characteristic time for the spin system to recover its equilibrium state completely. The magnetic-field increments were 0.04 mT for the center part of the spectrum with a 5 mT

width and 0.04–0.15 mT for the remaining part. The echo-detected ESR spectrum is equivalent to the absorption spectrum of conventional continuous-wave (cw) ESR, although the baselines of echo-detected ESR spectra are much flatter than those of cw ESR spectra.[19,24] This enables us to observe clear ^{29}Si hf structures of the LESR spectrum. All echo-detected ESR spectra were measured with a home-built pulsed ESR spectrometer with a microwave frequency of 11 GHz. This frequency was more useful for the deconvolution than the usual 9.2 GHz (X band), because overlapping of the two signals of $g = 2.004$ and 2.01 decreases as the resonant microwave frequency increases.[6,22] The details of our pulsed ESR spectrometer were described in previous papers.[24,25] The spin echo was generated by microwave pulses 17 and 34 nsec wide for 90° and 180° pulses, respectively, whose magnetic-field strength was estimated to be about 0.52 mT. The echo intensity was accumulated with a 50-nsec-wide boxcar gate and was then digitized with a 12-bit analog-to-digital converter.

Sample temperatures were controlled from 4.5 to 300 K using an Oxford ESR-900 system, and were measured by a thermocouple in the sample tube. The LESR intensity increases monotonically with decreasing temperature in addition to the contribution of the Boltzmann factor.[19] On the other hand, the number of echo signals accumulated was limited by the long repetition time due to a rapid increase in T_1. The best temperature for getting a high signal-to-noise ratio was found to be around 30 K.

LESR measurements were carried out using a Ti-sapphire laser ($h\nu = 1.7$ eV). The laser light was radiated into a microwave cavity through a glass fiber. The light intensity on the sample was adjusted to be 30 mW/cm^2, unless noted otherwise. We checked the time evolution of the LESR spectra and confirmed that there was no appreciable influence of photodegradation on any LESR spectrum.

Some of the ESR spectra were measured using a cw ESR spectrometer (Bruker ESP300E) with microwave frequencies of 3 and 34 GHz. These cw ESR measurements were carried out at 50 K using a field-modulation frequency of 100 kHz, modulation amplitude of 0.3–0.7 mT, and microwave power of 0.9–7.8 mW.

III. RESULTS

A. Spin-lattice relaxation time

Figure 1(a) shows spin-lattice relaxation curves at 30 K of the undoped sample ($p = 9.1$ at. %). Solid and open circles were measured at magnetic fields of 389.0 and 391.8 mT where the echo signals originate mainly from $g = 2.004$ and 2.01 signals, respectively [see Fig. 1(b)]. These curves were obtained by a pulse sequence of three-pulse inversion recovery (180° pulse$-t-$90° pulse$-\tau-$180° pulse$-\tau-$echo, $\tau = 240$ nsec, t is scanned, RT = 30 msec).[24] Solid lines in the figure represent fitted curves with stretched-exponential functions $I(t)/I(0) = 1 - 2\exp[-(t/T_1)\beta]$, where T_1 is the spin-lattice relaxation time and β is a dispersion parameter ($0 \leq \beta \leq 1$).[24] Values of T_1 and β at 30 K for $g = 2.004$ and 2.01 are summarized in Table II. It is found that T_1 of $g = 2.004$ is about three times longer than that of $g = 2.01$. This may reflect a difference in electronic structures between conduction- and valence-band-tail spins, which will be dis-
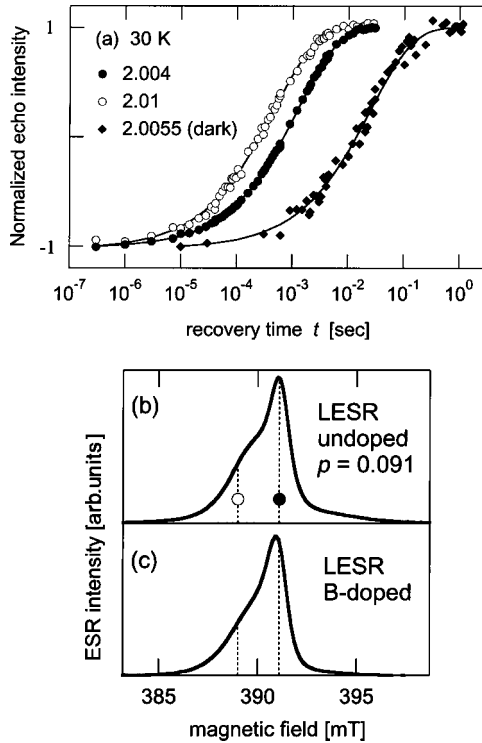
FIG. 1. (a) Echo recovery curves of the $g = 2.004$, 2.01, and 2.0055 signals at 30 K. Echo intensities are scaled from -1 to 1. LESR spectra of the (b) undoped and (c) B-doped a-Si:H samples. Dashed lines indicate magnetic fields at which we have measured the echo recovery curves. Symbols there correspond to those in 1(a).

cussed in Sec. IV A. Such a T_1 difference was also observed in the conduction- and valence-band-tail spins of P- and B-doped a-Si:H and a-Ge:H, respectively, although the two centers were separately observed in different samples.[26]

As seen in Fig. 1(a), the dark ESR signal of $g = 2.0055$ has a much longer T_1 than the above two: $T_1 = 26$ msec. The same relation was also found in illuminated conditions.[27] Using B-doped a-Si:H, we measured the 2.0055 signal and its T_1 under strong (100 mW/cm^2) illumination [Fig. 1(c)]. This 2.0055 signal is thought to arise from neutral DB's via an electron trapping process at positively charged DB's. The T_1 value of $g = 2.0055$ is six times longer than that of the coexistent 2.01 signal (Table II). Taking advantage of this feature, it is quite possible to reduce the 2.0055 component in

TABLE II. Spin-lattice relaxation parameters of the spin centers. B_r represents magnetic fields at which we have measured relaxation curves.

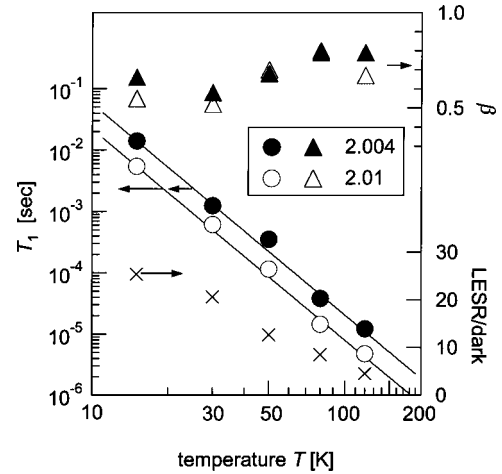| Experimental conditions	g	B_r (mT)	T_1 (msec)	β
undoped, $p = 9.1$ at. % (30 K)				
In the dark	2.0055	391.1	26	0.58
Under illumination	2.01	389.0	0.47	0.61
	2.004	391.8	1.3	0.59
B-doped (50 K)				
Under illumination	2.01	389.0	0.06	0.59
	2.0055	391.1	0.38	0.69

FIG. 2. Temperature dependence of T_1 (circles) and β (triangles). The data were obtained for undoped a-Si:H with $p = 4.7$ at. %. Solid lines indicate the dependence $T^{-3.4}$. ''LESR/dark'' represents the ratio of peak heights of the LESR spectrum to the dark ESR spectrum.

the LESR spectrum. The 2.0055 component should be decreased if we apply RT just long enough for the 2.004 and 2.01 components to recover to the equilibrium states (for example, 10 msec at 30 K), because such a RT is not sufficient for full recovery of the longer-T_1 component, $g = 2.0055$.

The dispersion parameter β is found in the range from 0.6 to 0.7 for every center (Table II). β values smaller than unity indicate that T_1 of each center has a distribution in the vicinity of the major value listed in Table II. This is reasonable because of the amorphous nature of the material. The distribution of T_1 values did not affect the echo-detected ESR experiments in the dark, shown by the fact that the shape of the dangling-bond signal was unchanged with varying RT. The shape of the LESR signals, however, was distorted when we adopted a RT much shorter than T_1. The distortion of the line shape was detected only in the center part of the spectra where $g = 2.004$ and 2.01 signals have considerable overlap. Such distortion is predominantly caused by the cross relaxation between the 2.004 and 2.01 spins rather than the T_1 distributions, because the cross relaxation is more effective in the overlapping region.[28]

The temperature dependence of T_1 and β is shown in Fig. 2. Generally, T_1 obeys a power-law dependence with respect to temperature T, i.e., $T_1 \propto T^{-m}$.[28] Actually, T_1 for both $g = 2.004$ and 2.01 obeyed a similar power law with $m \approx 3.4$ from 15 to 120 K, slightly different from $m = 2-3$ for doped a-Si:H from 30 to 100 K.[26] The value of 3.4 is difficult to understand from simple models for the spin-lattice relaxation process.[28] Peak heights of LESR spectra normalized to those of dark ESR spectra are also shown in the figure. Since the LESR intensity is much greater than the dark ESR intensity, the contribution of $g = 2.0055$ to T_1 is not observable.

B. ^{29}Si hyperfine structure of the LESR spectrum

Figure 3 shows LESR spectra of undoped samples with $p = 1.6$, 4.7, and 9.1 at. %, which were obtained by the two-pulse Hahn echo sequence with RT of 10 msec. Spin densi-
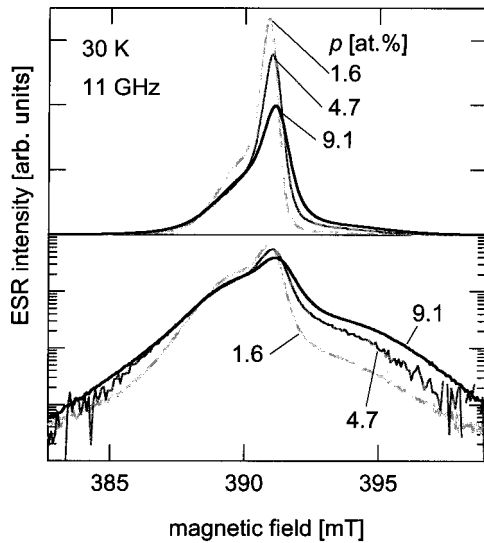
FIG. 3. ^{29}Si concentration dependence of the LESR spectrum of undoped a-Si:H. Intensities of those spectra are normalized to their areas. The upper and lower figures are linear and logarithmic plots, respectively.

ties of these spectra were found to lie within the range from 8×10^{16} to 1.0×10^{17} cm^{-3}, more than 20 times larger than those of the dark ESR signals obtained by the same pulse sequence. When the light intensity is sufficiently high, as in the present case, LESR spectra no longer depend on the relative intensity between the LESR and the dark ESR signals, although under very weak illumination (or at relatively high temperatures) LESR spectra seem to be influenced by the dark ESR component.[29,30] This means that there is no substantial contribution of the dark ESR component to the observed LESR spectrum for the strong-illumination cases.

With increasing ^{29}Si concentration, it was found that the peak height of $g = 2.004$ was reduced considerably. This is due to a signal broadening of the $g = 2.004$ signal induced by unresolved ^{29}Si hf splittings, which is effective for the $g = 2.004$ signal because of its narrow linewidth. An apparent shift in the peak position of the 2.004 signal is also a consequence of the reduction in the peak height of $g = 2.004$ relative to $g = 2.01$. The ^{29}Si concentration dependence shown here indicates that excessive doping of ^{29}Si in the film causes extreme signal broadening, which smears out the separation between the 2.004 and 2.01 signals as well as ^{29}Si hf splittings.

As seen in the logarithmic plot of Fig. 3, there is a weak and broad signal in the tail region of every LESR spectrum. These signals are high-magnetic-field-side ^{29}Si hf lines, because the area ratio $S_{\text{high-hf}}$, of these lines to the total spectrum increased proportionally to p, as seen in Fig. 4(a). The deconvolution of the high-field-side hf lines was performed by extrapolating a tail curve from the main peak of $g = 2.004$, in which we assumed an exponential decay of the tail.[22] Likewise, in Fig. 4(b), the $S_{\text{high-hf}}$ values are estimated for the dangling-bond signal of $g = 2.0055$. Solid lines represent the relation $S_{\text{high-hf}} = p/2$, which corresponds to the fact that the wave function of the neutral DB center is localized mainly on a single Si atom.[12–14] A good coincidence between the line and plots in Fig. 4(b) assures the validity of the deconvolution of high-field hf lines. For the LESR spec-
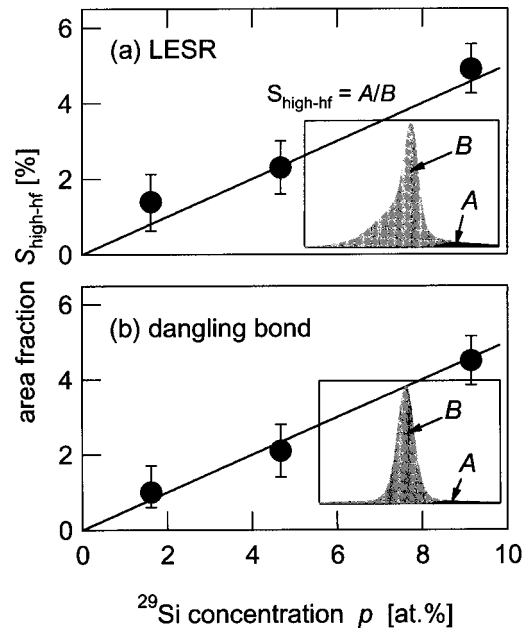

FIG. 4. ^{29}Si concentration dependence of the area fraction ($S_{\text{high-hf}}$) of the high-field-side ^{29}Si hf line: (a) for LESR and (b) for dark ESR spectra. $S_{\text{high-hf}}$ is given by the area ratio A/B.

trum, $S_{\text{high-hf}}$ seems to trace a similar line as in the dangling-bond case. Previously, Yamasaki *et al.*[19] tentatively suggested that the wave function of the LESR spin centers is localized on a single Si atom, simply because the value of $S_{\text{high-hf}}$ was close to $p/2$ for $p = 4.7$ at. % [see Fig. 4(a)]. However, the data are not sufficient to discuss, because the LESR spectrum is composed of two signals ($g = 2.004$ and 2.01). In order to obtain more detailed and correct information, it is necessary to deconvolute the LESR spectrum into the two signals. Fortunately, by taking advantage of the difference in T_1 between the two LESR centers (see Sec. III A), it is quite possible to experimentally deconvolute the LESR spectrum, as we reported previously.[22]

Figure 5 shows the result of the experimental deconvolution for $p = 4.7$ at. % (a natural-abundance sample). The "total" spectra in Figs. 5(a) and 5(b) were measured by echo-detected ESR techniques using a two-pulse Hahn echo (RT = 0.5 msec) and a three-pulse stimulated echo (90° pulse–τ–90° pulse–τ'–90° pulse–τ–echo, $\tau = 240$ nsec, $\tau' = 1$ msec, RT = 10 msec), respectively. τ' longer than 1 msec was not effective because of a serious reduction of the echo intensity. The details of the deconvolution procedure have been reported in Ref. 22. The center part of the LESR spectra could not be deconvoluted completely because of the distortion of the spectra as discussed in the preceding section. Figure 5 clearly demonstrates that the ^{29}Si high-field-side hf line of the LESR spectrum is related mainly to the 2.004 signal, which is the most important feature. Peak positions of the two deconvoluted signals were found to correspond to $g = 2.004$ and 2.01, respectively. The area ratio of the deconvoluted two signals was estimated to be [2.004]:[2.01] ≈ 1.3:1 for the normal LESR spectrum shown in Fig. 3. The same results were also obtained for a ^{29}Si-enriched sample ($p = 9.1$ at. %).[22] For a ^{29}Si-diluted sample ($p = 1.6$ at. %), it was rather difficult to get sufficient intensity of the ^{29}Si structure after the deconvolution process.
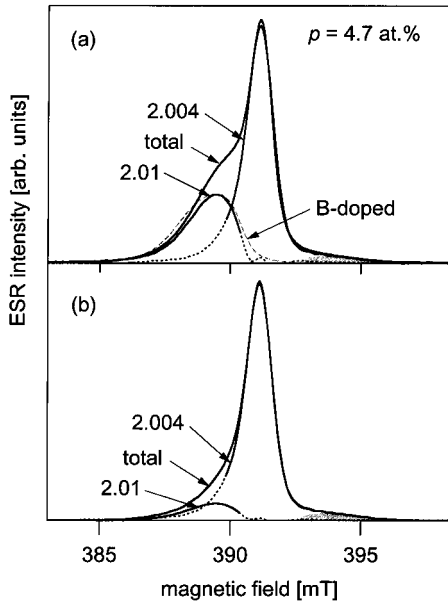
FIG. 5. Experimental deconvolution of two LESR signals for the case of $p = 4.7$ at. %. Solid lines indicate the deconvoluted 2.004 and 2.01 spectra with high reliability in data analyses, while dashed lines include some ambiguity. Shaded regions show the high-field-side hf structure of ^{29}Si. The dark ESR spectrum of B-doped a-Si:H is also shown by a broken line.

C. Electronic structure of LESR centers

In this section, we extract detailed information about the electronic structures of LESR centers from the deconvoluted ^{29}Si hf structures. One of the most important pieces of information is the area fraction S_{hf} of the entire ^{29}Si hf structure (a group of low- and high-field-side hf lines) in the deconvoluted signal. The quantity S_{hf} is determined by the number of Si atoms, N, on which an electron spin is mainly located. When $N = 1$, S_{hf} equals simply $p/2 + p/2 = p$, as is illustrated in Fig. 6(a). For any N, since the probability that all N Si atoms have no nuclear spin is $(1-p)^N$, S_{hf} should be given by $1 - (1-p)^N$. Although this includes the small probability of ^{29}Si hf lines overlapping on a central line, e.g., a probability of $p^2/2$ for the $N = 2$ case shown in Fig. 6(b), such a small probability is negligible for the case of small N and p. The value of S_{hf} is experimentally determined by the area ratio A/B of the deconvoluted signal, as shown in Fig. 6(c). The area B is calculated using the high-field-side half of the deconvoluted 2.004 spectrum in order to eliminate an ambiguity in the ''dashed-line'' region (cf. Fig. 5). The high-field-side ^{29}Si hf structure was estimated by the procedure used in Sec. III B. As a result, the S_{hf} values were estimated to be 0.20 ± 0.03 and 0.09 ± 0.03 for $p = 0.091$ and 0.047, respectively. Thus, for the 2.004 center,

$$N = \begin{cases} 2.3 \pm 0.4 & \text{for } p = 0.091 \\ 2.1 \pm 0.4 & \text{for } p = 0.047. \end{cases} \quad (1)$$

Consequently, it is concluded that the wave function of the 2.004 center spreads mainly over two Si atoms.[22] In the above discussion, we assumed that the wave function of the spin center spreads over N Si atoms uniformly, although the actual wave function may fluctuate among N Si atoms. A more exact analysis needs to consider variations of ^{29}Si hf
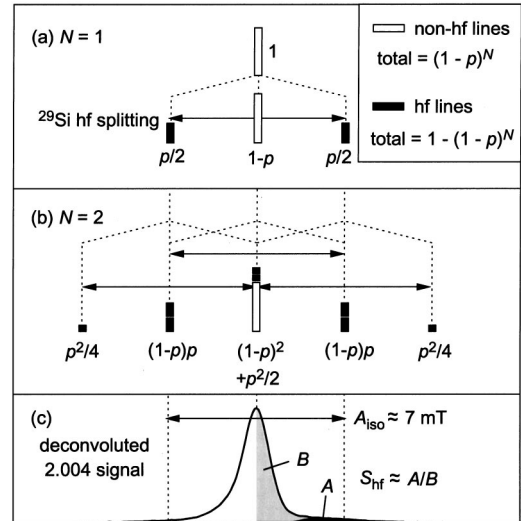

FIG. 6. Schematic views of ^{29}Si hf splitting for cases of (a) $N = 1$ and (b) $N = 2$, assuming two equivalent hf splittings. (c) Estimation of S_{hf} and A_{iso} for the deconvoluted 2.004 signal.

interactions among N Si atoms. However, the fluctuation contributes only to the linewidth of the hf structure and therefore does not affect the above conclusion.

Another interesting feature is the isotropic hf splitting A_{iso}, which arises mainly from the $3s$ character in the wave function of a spin center.[12–14] As is shown in Fig. 6(c), the isotropic hf splitting is estimated to be

$$A_{iso} \approx 7 \text{ mT} \quad \text{for } g = 2.004. \quad (2)$$

In contrast to the 2.004 signal, the 2.01 signal did not appear to show hf structure. Therefore, the isotropic hf splitting of $g = 2.01$ should be smaller than that of $g = 2.004$. The 2.01 signal in B-doped a-Si:H [Fig. 5(a)] also shows no discernible hf structures.[21] Furthermore, both the 2.01 signals are similar in their asymmetric line shape. The origin of the asymmetric line shape of $g = 2.01$ is ascribed either to the powder pattern[31] due to anisotropy of the g value, or to the convolution of hf structures. To clarify the origin, ESR spectra of $g = 2.01$ were measured at microwave frequencies (ν) of 3,11,34 GHz, and are shown in Fig. 7(a). In the figure, although the linewidth was reduced by less than 1.0 mT in the 3 GHz spectrum, distortion of the spectral shape due to isotropic hf interactions was still not observed. This means that the isotropic hf splittings of $g = 2.01$ are smaller than 3 mT, i.e.,

$$A_{iso} < 3 \text{ mT} \quad \text{for } g = 2.01, \quad (3)$$

and hence the asymmetric line shape of $g = 2.01$ originates from the powder pattern. In Fig. 7(b), ESR intensities are plotted as a function of g value. The asymmetry in the line shape is enhanced in the 34 GHz spectrum in Fig. 7(b), which clearly indicates a convolution of the powder pattern. To estimate principal g values of the 2.01 signal, we carried out a powder-pattern simulation of the 2.01 spectra. In the simulation, an ideal powder pattern[31] was broadened by convoluting the Voigt broadening function with the full width at half maximum, W, and a shape parameter y.[14] We assumed
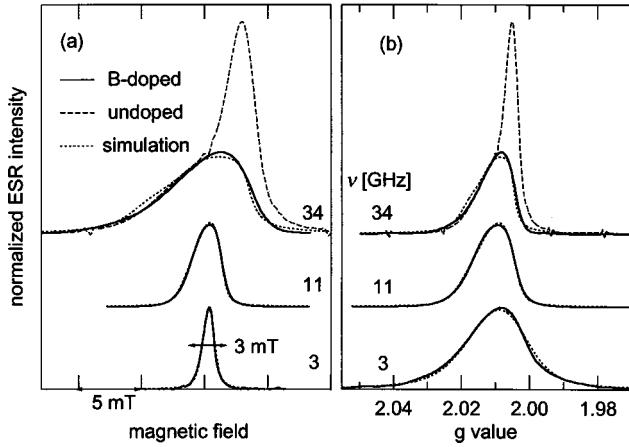
FIG. 7. Multifrequency (3,11,34 GHz) ESR measurements on the $g=2.01$ signal in B-doped a-Si:H (solid lines). ESR intensities are plotted (a) as a function of applied magnetic field B, and (b) as a function of g value, where $g=[71.4488\nu\,(\text{GHz})]/[B(\text{mT})]$. The 2.01 spectra are normalized to their peak heights and are vertically shifted for clarity. Dashed lines indicate simulated powder-pattern spectra. LESR spectra in undoped a-Si:H ($p=9.1$ at. %) for 34 GHz are also shown by broken lines, with intensities modified to fit their 2.01 signals approximately to the B-doped 2.01 signal.

that the width W is proportional to the g shift (Δg) from the free-electron g value (2.0023) as well as the resonant frequency, because such a dependence has been observed in the dangling-bond spectrum in a-Si:H.[14] The fitting parameters were g_1, g_2, and g_3 (principal g values $g_1>g_2>g_3$), W_0 and W_1 (width parameters: $W\equiv W_0+W_1\Delta g\,\nu$), C (normalizing constant), and y, where g_1, g_2, g_3, W_0, and W_1 were set to be common for all the spectra. The simulation minimized the sum of deviations among three experimental and fitted spectra using the same algorithm as in previous work.[14] The best-fitted spectra (dashed lines in Fig. 7) were obtained for $g_1\approx2.019$, $g_2\approx2.012$, and $g_3\approx2.005$. One of the g values (g_3) was close to $g=2.004$, so the two LESR signals of $g=2.004$ and 2.01 were not completely separated even in the 34 GHz spectrum, as shown in Fig. 7.

It has been reported that the energetic positions in the gap are deeper for valence-band-tail holes than for conduction-band-tail electrons, resulting in stronger localization for $g=2.01$ centers than $g=2.004$ ones.[3,8,32] The stronger localization must cause larger isotropic splitting, unless the wave function of the spin center has less $3s$ component. Thus, the weaker isotropic hf interaction of $g=2.01$ means that the wave function of the 2.01 center has much less $3s$ component compared to the 2.004 center; in other words, it consists of $3p$ component predominantly. This difference will be interpreted later in terms of the origin of the LESR centers. Although the 2.01 center has much $3p$ component, it is difficult to detect the anisotropic ^{29}Si hf interactions in the 2.01 spectrum, because a 100% localized $3p$ orbital of the ^{29}Si atom causes an anisotropic hf splitting of no more than 3.6 mT.[33]

The electronic levels that are located in the vicinity of the mobility gap of a-Si:H are characterized by a combination of $3s$ and $3p$ levels of Si atoms. Thus, to consider the electronic structures of band-tail states, it is useful to describe the wave function ψ of $g=2.004$ and 2.01 by a linear combination of atomic orbitals. That is $\psi=\Sigma_i\alpha_i(\sigma_i|3s\rangle+\pi_i|3p\rangle)$, where $|3s\rangle$ and $|3p\rangle$ denote the atomic $3s$ and $3p$ orbitals of Si, i indexes all Si atoms within the extent of ψ, α_i^2 represents the degree of localization of an unpaired electron on site i, and σ_i^2 and π_i^2 are fractions of $3s$ and $3p$ orbitals on site i, respectively.[12,14] The projection coefficients satisfy the normalization conditions $\Sigma_i\alpha_i^2=1$ and $\sigma_i^2+\pi_i^2=1$ for all i. The isotropic hf splitting A_{iso} has been theoretically calculated to be 149.0 mT for a 100% localized $3s$ orbital of ^{29}Si atom.[33] Comparing Eq. (2) with this value, the $3s$ component in the wave function of the 2.004 center is estimated to be $7/149=5\%$ on each of the two Si atoms. On all other i sites, the $3s$ components should be much smaller than 5%. Therefore,

$$\alpha_1^2\sigma_1^2\approx\alpha_2^2\sigma_2^2\approx0.05,$$
$$\alpha_i^2\sigma_i^2<0.05\quad(i\neq1,2) \tag{4}$$

for $g=2.004$, where $i=1$ and 2 represent the two Si atoms counted in N. For the 2.01 center, all $\alpha_i^2\sigma_i^2$ should be smaller than $3/149=2\%$, because $A_{\text{iso}}<3$ mT [Eq. (3)], namely,

$$\alpha_1^2\sigma_1^2<0.02\quad\text{for all }i \tag{5}$$

for $g=2.01$. The localization coefficients α_1^2 and α_2^2 for $g=2.004$ should be larger than those for $g=2.01$, as we mentioned above. Thus, to satisfy Eqs. (4) and (5), σ_1^2 and σ_2^2 for $g=2.01$ should be much smaller than those for $g=2.004$,

$$\sigma_1^2,\sigma_2^2\quad(\text{for }g=2.01)\ll\sigma_1^2,\sigma_2^2\quad(\text{for }g=2.004). \tag{6}$$

A further evaluation of the projection coefficients has been reported in Ref. 22.

IV. DISCUSSION

A. Origin of LESR centers

For the origin of the LESR centers, two models have so far been proposed. In this section, those models are compared with the ESR results obtained here, in particular, with Eqs. (1) and (6).

One model is that of electrons or holes trapped at weak Si-Si bonds.[34] In an amorphous network, it is quite possible that greatly elongated covalent bonds (weak bonds) are present and give rise to the energy levels in the band-tail regions. In this case, an electron is trapped in an antibonding state and its wave function extends over the two Si atoms associated with the weak Si-Si bond. In the other model, electrons and holes are trapped at positively and negatively charged DB's with negative U, resulting in neutral DB's with $g=2.004$ and 2.01, respectively.[17–20] The resultant neutral DB's are thought to be similar to those observed in the dark. However, a neutral DB state is characterized by an electron localized on a single Si atom (namely, $N\approx1$),[12–14] which is clearly inconsistent with the present result of $N\approx2$ [Eq. (1)]. Consequently, the present results suggest that the origin of the LESR center of $g=2.004$ is electrons trapped at weak Si-Si bonds located at the conduction-band-tail rather than electrons trapped at positively charged DB's.

It is reasonable to consider for the $g=2.01$ center, by analogy with the 2.004 center, that it originates from holes trapped in the bonding states of the weak Si-Si bonds located in the valence-band tail. The weak Si-Si bond model can explain why the 2.01 center has less $3s$ component in its wave function than the 2.004 center [cf. Eq. (6)]. As in crystalline silicon, the top of the valence band and the bottom of the conduction band in a-Si:H are characterized by $3p$ orbital ($p\sigma$ state) and an admixture of $3s$ and $3p$ orbitals ($sp\sigma^*$ state), respectively.[35] The antibonding and bonding states of the weak Si-Si bond retain essentially similar features to normal Si-Si bonds. Therefore, the wave function of holes trapped in the bonding states of the weak bonds will consist of much less $3s$ component than that of electrons in the antibonding levels, resulting in smaller isotropic hf splitting of $g=2.01$.

The above discussion is supported by more quantitative evaluations. Takeda $et~al.$ reported a first-principles local-density-functional calculation of a weak bond with 27% stretching embedded in polysilane chains (Si_4H_8 and Si_6H_{12}).[36] They showed that holes localize at the center of the weak bond and the hole wave function is composed mainly of $3p$ orbital, while electrons tend to localize at two Si atoms of the weak bond and its wave function has a $3s$ component. As a result, the isotropic hf splitting of the hole center was calculated to be less than $\frac{1}{70}$ of that of the electron center. The energy separation between the two weak-bond levels was estimated to be 65% of the energy gap for polysilane chains ($=3.9$ eV), which is comparable with the actual range between 60% and 100% of 1.7 eV in a-Si:H.[1,2,8] More recently, Ishii and Shimizu calculated ^{29}Si hf interactions in negatively and positively charged weak bonds with 50–75% stretching by means of the density-functional method for clusters with 8–26 Si atoms.[37] They found that the isotropic hf splitting for the negatively charged weak bond becomes 6–11 mT as against 0.1–0.2 mT for the positively charged one, which is quite consistent with our experimental results.

Note that any s orbitals make little contribution to the spin-orbit interaction, because their orbital angular momentum is zero.[38] Thus, due to more $3s$ component in the wave function of $g=2.004$, the 2.004 center tends to generate less spin-orbit coupling, resulting in a longer T_1 and smaller g shift compared to the 2.01 center. Such a trend is consistent with the T_1 difference and the g shift observed in the experiment.

In contrast to the weak bond, charged DB's are unlikely to adopt different isotropic hf splittings between $g=2.004$ and 2.01. As is seen in Fig. 1(c) for the case of positively charged DB's, both positively and negatively charged DB's are probably converted to neutral DB's with isotropic hf splitting close to 7 mT.

A detailed study of the electron-spin-echo envelope modulation revealed that the LESR centers are spatially separated from hydrogen atoms by approximately 0.4 nm.[25] This is quite reasonable for the weak Si-Si bond model, because insertion of hydrogen in a disordered Si network may relax local stress and prevent the formation of elongated covalent Si-Si bonds near hydrogen atoms. Conventional a-Si:H films contain other impurities such as oxygen, carbon, and nitrogen with concentrations of 10^{18}–10^{20} cm^{-3}.[39] However, a high-purity undoped film, which contains no

TABLE III. Comparison of data for conduction-band-tail electrons from the present LESR and the previous PL and ODMR (Refs. 40–42, 44) experiments.

	LESR	PL and ODMR
Spatial extent	smaller than 1 nm	≈ 1 nm
Time constant of decay	$>10^2$ sec	$\approx 10^{-3}$ sec
g value	2.004	≈ 1.99
Concentration	$\leq 10^{17}$ cm^{-3}	$\geq 10^{18}$ cm^{-3}
Energy positions	deep	shallow
Origin of trap center	weak Si-Si bond	?

more than 10^{16} cm^{-3} of impurities, still reveals the band-tail structure in its optical absorption spectrum.[39] Therefore, we speculate that the impurities do not directly relate to the formation of weak bonds, and thus the weak bond may be an intrinsic structure of the amorphous silicon network.

B. Comparison between LESR centers and other band-tail states

Our experiment revealed that the $g=2.004$ electrons generate only two main isotropic hf interactions of ^{29}Si. On the other hand, previous photoluminescence (PL) and spin-dependent PL [the so-called optically detected magnetic resonance (ODMR)] experiments suggested that the spatial extent of the conduction-band-tail electrons is as large as 1 nm.[40,41] Those experiments analyzed the PL signal at a photon energy of 1.2–1.4 eV which has been attributed to the radiative recombination between conduction-band-tail electrons and valence-band-tail holes.[7,40,42] Normally, a sphere of 1 nm radius in a-Si:H (Si density $\approx 5\times 10^{22}$ atoms/cm^{-3}) contains more than 150 Si atoms.[43] Thus, the PL electrons are considered to have substantial electron densities on several dozen Si atoms and therefore do not adopt the same ^{29}Si hf interactions as the 2.004 electrons.

In order to interpret the difference between the LESR and PL data, we considered that the band-tail electrons observed in the PL possess relatively higher energetic positions and larger spatial extent compared to the 2.004 electrons in LESR. This speculation is consistent with various experimental facts, which are summarized in Table III. (1) The time constant of the decay is quite different between the two experiments; below 50 K, the PL intensity decays with a time constant of 10^{-3} sec after excitation,[40] but for the LESR intensity, the constant is larger than 10^2 sec. The much slower decay for the LESR may be ascribed to the deeper energy location of the 2.004 electrons. Since the PL intensity decreases proportionally with the rate of radiative recombination, it is quite difficult for PL to detect the 2.004 electrons, which have a very long recombination lifetime. (2) The g value is quite different; a time-resolved ODMR measurement under intense pulsed excitations (peak power ≈ 220 kW/cm^2) detected a very weak signal of $g\approx 1.99$ which was tentatively ascribed to band-tail electrons,[44] but such a signal is similar to a conduction-electron resonance in microcrystalline silicon[45] ($g=1.998$) rather than $g=2.004$. This suggests that the PL electrons are located in shallow levels close to the mobility edge. (3) The carrier concentration is different; the concentration of the PL electrons is eas-

ily higher than 10^{18} cm^{-3},[40] while that of the 2.004 electrons did not exceed 10^{17} cm^{-3}.[30] It also leads to higher-energy positions for the PL electrons. Further, this fact suggests that the 2.004 centers relate to only a part of the conduction-band-tail states, although the PL electrons may be responsible for the major part.

The reason that LESR and PL revealed different conduction-band-tail electrons is tentatively ascribed to the following features of the LESR. The LESR measurements are efficient in detecting band-tail electrons having a long recombination lifetime (τ_r), because the steady-state density N of band-tail electrons should increase as τ_r increases (note that the steady-state rate equation $dN/dt = G - N/\tau_r = 0$, where G is the generation rate of band-tail electrons, results in $N = G\tau_r$). In addition, it is also required that unpaired spins have a T_1 long enough to avoid a serious reduction in the ESR signal intensity due to lifetime broadening. Naturally, localized electrons in deeper band-tail levels have longer τ_r (and may also have longer T_1) as compared to delocalized electrons in shallower band-tail levels. Therefore, LESR will be increasingly effective for deeper band-tail levels, resulting in smaller spatial extent for the LESR electrons than for the PL ones.

As mentioned earlier, the ^{29}Si hf structure of the PL electrons may be different from that of the LESR electrons. For example, discernible ^{29}Si hf splitting might be absent in the ODMR spectrum due to the delocalization of unpaired electrons. Unfortunately, previous experimental results as well as the present work are not sufficient to determine what sort of structural fluctuation causes such weakly localized centers, with a spatial extent of 1 nm, having a density of states higher than 10^{18} cm^{-3}. For the weak-bond center, theoretical calculations suggest 0.3–0.4 nm for the Si-Si bond length.[36,37,46] Weak Si-Si bonds whose Si-Si bond length is closer to a normal Si-Si length (0.235 nm) than to 0.3 to 0.4 nm might be one of the origins of the weakly localized centers. But even so, many kinds of structural fluctuation will contribute to the formation of the centers because of their large spatial extent. For example, it was reported that fluctuations of either bond-angle or ring statistics rather than bond length are effective in generating band-tail states.[47] Thus, the nature of the weakly localized centers is probably different from that of the 2.004 center.

V. SUMMARY

This paper follows up our previous work[22] with more complete experimental data and discussion. We have investigated the electronic and microscopic structures of the LESR centers of $g = 2.004$ (conduction-band-tail electrons) and 2.01 (valence-band-tail holes) in undoped a-Si:H on the basis of detailed analyses of their ^{29}Si hf structures. In this study, we took advantage of pulsed ESR techniques, samples with different content of ^{29}Si (1.6, 4.7, 9.1 at. %), and multifrequency (3–34 GHz) ESR studies, and obtained experimental results as follows.

(1) The T_1 of the $g = 2.004$ center is about three times longer than that of $g = 2.01$ (Sec. III A). Using the T_1 difference, the LESR spectra can be experimentally deconvoluted into two independent signals for $g = 2.004$ and 2.01 (Sec. III B).

(2) The fractional intensity of the ^{29}Si hf structure in the deconvoluted signal of $g = 2.004$ revealed that the wave function of the 2.004 center spreads mainly over two Si atoms (Sec. III C). This suggests that the origin of the 2.004 center is electrons trapped in the antibonding states of the weak Si-Si bond rather than those trapped in the positively charged DB's (Sec. IV A). By analogy, we suggested that the 2.01 center arises from holes trapped in the bonding states of the weak Si-Si bond.

(3) The ^{29}Si isotropic hf splitting of $g = 2.004$ was estimated to be around 7 mT, while that of $g = 2.01$ was below 3 mT (Sec. III C). This indicates that the wave function of $g = 2.01$ consists mainly of the $3p$ component, while the wave function of $g = 2.004$ has more $3s$ component compared to the 2.01 center. The difference can be accounted for within the framework of the weak-bond model (Sec. IV A).

(4) The anisotropic line shape of $g = 2.01$ originates from a large anisotropy of the g value (Sec. III C).

(5) We discussed the difference in the nature of band-tail electrons observed in LESR and PL experiments on the basis of our results and other experimental findings (Sec. IV B). The discussion pointed out that the 2.004 electrons are presumably more localized and are located in deeper band-tail levels than the PL electrons.

*Present address: System Devices and Fundamental Research, NEC Corporation, Tsukuba, 305-8501, Japan.

[1] S. Yamasaki, Philos. Mag. B **56**, 79 (1987).

[2] S. Aljishi, J. D. Cohen, S. Jin, and L. Ley, Phys. Rev. Lett. **64**, 2811 (1990).

[3] T. Tiedje, J. M. Cebulka, D. L. Morel, and B. Abels, Phys. Rev. Lett. **46**, 1425 (1981); W. E. Spear and C. S. Cloude, Philos. Mag. B **58**, 467 (1988); M. Kemp and M. Silver, *ibid.* **63**, 437 (1991).

[4] K. Hattori, H. Okamoto, and Y. Hamakawa, J. Non-Cryst. Solids **198-200**, 288 (1996).

[5] J. C. Knights, D. K. Biegelsen, and I. Solomon, Solid State Commun. **22**, 133 (1977).

[6] H. Dersh, J. Stuke, and J. Bachelor, Phys. Status Solidi B **105**, 265 (1981).

[7] R. A. Street, D. K. Biegelsen, and R. L. Weisfield, Phys. Rev. B **30**, 5861 (1984).

[8] M. Stutzmann, D. K. Biegelsen, and R. A. Street, Phys. Rev. B **35**, 5666 (1987).

[9] S. G. Bishop, U. Strom, and P. C. Taylor, Phys. Rev. Lett. **34**, 1346 (1975); **36**, 543 (1976).

[10] R. A. Street and N. F. Mott, Phys. Rev. Lett. **35**, 1293 (1975).

[11] M. Kastner, D. Adler, and H. Fritzsche, Phys. Rev. Lett. **37**, 1504 (1976).

[12] M. Stutzmann and D. K. Biegelsen, Phys. Rev. B **40**, 9834 (1989); in *Amorphous Silicon and Related Materials*, edited by H. Fritzsche (World Scientific, Singapore, 1988), pp. 557–594.

[13] N. Ishii and T. Shimizu, Phys. Rev. B **42**, 9697 (1990).

[14] T. Umeda, S. Yamasaki, J. Isoya, and K. Tanaka, Phys. Rev. B **59**, 4849 (1999).

[15] J. D. Cohen, J. P. Harbison, and K. W. Wecht, Phys. Rev. Lett. **48**, 109 (1982).

[16] H. Okamoto and Y. Hamakawa, Solid State Commun. **24**, 1197 (1977).

[17] D. Adler, Sol. Cells **9**, 133 (1983).

[18] K. Morigaki, J. Phys. Soc. Jpn. **50**, 2279 (1981).

[19] S. Yamasaki, H. Okushi, A. Matsuda, K. Tanaka, and J. Isoya, Phys. Rev. Lett. **65**, 756 (1990).

[20] N. Orita, T. Matsumura, and H. Katayama-Yoshida, J. Non-Cryst. Solids **198-200**, 347 (1996).

[21] S. Yamasaki, S. Kuroda, J. Isoya, and K. Tanaka, J. Non-Cryst. Solids **97-98**, 691 (1987).

[22] T. Umeda, S. Yamasaki, J. Isoya, A. Matsuda, and K. Tanaka, Phys. Rev. Lett. **77**, 4600 (1996).

[23] S. Yamasaki, Electrotecnical Laboratory Research Report No. 883, 1987 (unpublished).

[24] J. Isoya, S. Yamasaki, A. Matsuda, and K. Tanaka, Philos. Mag. B **69**, 263 (1994).

[25] J. Isoya, S. Yamasaki, H. Okushi, A. Matsuda, and K. Tanaka, Phys. Rev. B **47**, 7013 (1993).

[26] M. Stutzmann and D. K. Biegelsen, Phys. Rev. B **28**, 6256 (1983).

[27] Under illumination, T_1 of $g = 2.0055$ can be decreased due to conversion between neutral and charged DB states, and also due to the cross relaxation between 2.0055 and 2.01 spins, which were discussed in Refs. 26 and 28, respectively.

[28] M. K. Bowman and L. Kevan, in *Time Domain Electron Spin Resonance*, edited by L. Kevan and R. N. Schwartz (Wiley, New York, 1979), pp. 67–106.

[29] G. Schumm, W. B. Jackson, and R. A. Street, Phys. Rev. B **48**, 14 198 (1993).

[30] T. Umeda, S. Yamasaki, J. Isoya, A. Matsuda, and K. Tanaka, J. Non-Cryst. Solids **227-230**, 353 (1998).

[31] P. C. Taylor, J. F. Baugher, and H. M. Kriz, Chem. Rev. **75**, 203 (1975).

[32] H. Dersh, J. Stuke, and J. Beichler, Phys. Status Solidi B **107**, 307 (1981).

[33] G. D. Watkins and J. W. Corbett, Phys. Rev. A **134**, 1359 (1964).

[34] M. Stutzmann, W. B. Jackson, and C. C. Tsai, Phys. Rev. B **32**, 23 (1985).

[35] W. B. Jackson, S. M. Kelso, C. C. Tsai, J. W. Allen, and S.-J. Oh, Phys. Rev. B **31**, 5187 (1985).

[36] K. Takeda, K. Shiraishi, M. Fujiki, M. Kondo, and K. Morigaki, Phys. Rev. B **50**, 5171 (1994).

[37] N. Ishii and T. Shimizu, Solid State Commun. **102**, 647 (1997).

[38] A. J. Stone, Proc. R. Soc. London, Ser. A **271**, 424 (1963).

[39] T. Kamei, N. Hata, A. Matsuda, T. Uchiyama, S. Amano, K. Tsukamoto, Y. Yoshioka, and T. Hirao, Appl. Phys. Lett. **68**, 2380 (1996).

[40] C. Tsang and R. A. Street, Phys. Rev. B **19**, 3027 (1979).

[41] M. Yoshida and K. Morigaki, J. Phys. Soc. Jpn. **58**, 3371 (1989).

[42] F. Boulitrop, Phys. Rev. B **28**, 6192 (1983).

[43] D. Weaire, N. Higgins, P. Moore, and I. Marshall, Philos. Mag. B **40**, 243 (1979).

[44] H. Takenaka, C. Ogihara, and K. Morigaki, J. Phys. Soc. Jpn. **57**, 3858 (1988).

[45] J. H. Zhou, S. Yamasaki, J. Isoya, K. Ikuta, M. Kondo, A. Matsuda, and K. Tanaka, in *Advances in Microcrystalline and Nanocrystalline Semiconductors—1996*, edited by R. W. Collins, P. M. Fauchet, I. Shimizu, J.-C. Vial, T. Shimada, and P. A. Alivisatos, MRS Symposium Proceedings No. 452 (Materials Research Society, Pittsburgh, 1997), p. 821.

[46] N. Ishii, M. Kumeda, and T. Shimizu, Phys. Status Solidi B **116**, 91 (1983).

[47] F. Yonezawa and M. H. Cohen, in *Fundamental Physics of Amorphous Semiconductors*, edited by F. Yonezawa (Springer-Verlag, Singapore, 1981), pp. 119–144.